

# Multifunctional PEC for Efficient Operation of Electric Vehicles with Dual Power Supplies

Shahla K T<sup>1</sup>, Sheela S<sup>2</sup>

<sup>1</sup>PG Scholar, Dept. of Electrical and Electronics Engineering, NSS College of Engineering, Palakkad, India

<sup>2</sup>Professor, Dept. of Electrical and Electronics Engineering, NSS College of Engineering, Palakkad, India

\*\*\*

**Abstract** - This paper deals with a Power Electronic Converter (PEC) which enables charging of a battery from both solar power and grid power. The dual power charging will increase the efficiency of the converter. For electric vehicle operations many conversion stages are required such as AC-DC rectification, MPPT converter stage and bidirectional DC-DC converter which can be integrated together by the introduction of an integrated converter. The number of components can be reduced by the placement of integrated converter. The Integrated Converter used can function in various vehicle modes such as charging from solar and grid modes, running mode and V2G/V2H operation mode. The vehicle battery can be charged from either solar power or grid power. The battery uses both power sources simultaneously when the power supply from solar source is not sufficient. The Integrated Power Converter acts as an isolated SEPIC converter during charging mode from grid power and as a non-isolated SEPIC converter in solar power charging mode. In propulsion and regenerative braking modes, it acts as boost topology and buck topology respectively. The Integrated Converter acts as a ZETA converter for Vehicle-to-Grid (V2G) mode.

**Key Words:** V2G, V2H, PEC, Electric vehicles, ZETA, SEPIC, MPPT Converter

## 1. INTRODUCTION

An electric vehicle (EV) is a vehicle that uses one or more electric motors or traction motors for propulsion. An electric vehicle may be powered through a collector system by electricity from off-vehicle sources, or may be self-contained with a battery, solar panels, fuel cells or an electric generator to convert fuel to electricity. During the last few decades, environmental impact of the petroleum-based transportation infrastructure, along with the fear of peak oil demand, has led to renewed interest in an electric transportation infrastructure. EVs differ from fossil fuel-powered vehicles in that the electricity they consume can be generated from a wide range of

sources, including fossil fuels, nuclear power, and renewable sources such as tidal power, solar power, hydropower, and wind power or any combination of those. The electric vehicles (EVs) battery chargers are classified as off-board chargers and on-board chargers. The On-Board charger system described in the material below converts the AC input from the grid to a DC input which charges the battery. An off-board battery charger is less constrained by size and weight and keeps redundancy in power electronic converters, which adds flexibility in the system.

The Bidirectional on-board chargers are broadly classified under single-stage and two-stage topologies. The commonly used single-stage topologies are half-bridge, full-bridge and multilevel converters. Most commonly used bidirectional AC-DC converters are half-bridge, full-bridge and multilevel converters. The modes of operations of EVs are mainly charging and running (Propulsion and Regenerative Braking). The charging of EVs can be made in different methods which is shown in Fig.1.

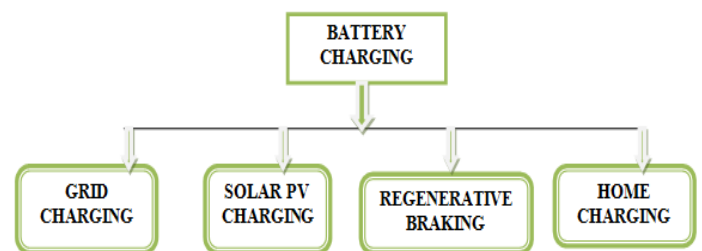


Fig.1: Multiple options for charging EVs

In conventional single-stage charging system, a bidirectional DC-DC converter is connected between DC-link of inverter and battery for power flow during Propulsion (PP) and Regenerative Braking (RB) modes. To charge the EV from solar PV and grid at least three converters are generally used. First, a DC-DC converter is utilized for maximum power point tracking (MPPT) operation of the solar PV. The output of solar PV (after

MPPT) is connected to the output of grid interfaced converter (second converter), which forms a DC-link, and then a bidirectional DC-DC converter (third converter) is connected between the DC-link and the battery. To eliminate this bidirectional DC-DC converter from single-stage charging system, power electronics researchers have proposed integrated type of chargers. In the integrated charger, the bidirectional DC-DC converter of conventional single-stage system connected between battery and DC-link is integrated with front-end converter at the cost of some additional switches. The overall integrated system has fewer number of total components compared to single-stage charging system. The block diagram of the conventional EV charging system is shown in Fig.2.

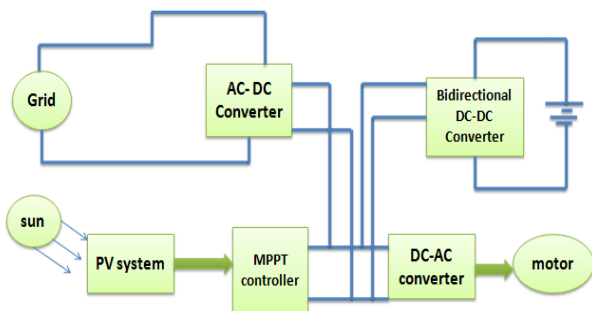


Fig.2: Block diagram of conventional EV charging system

This project deals with a Power Electronic Converter (PEC) which enables charging of a battery from both solar power and grid power. The Integrated Converter used can function in various vehicle modes such as charging from solar and grid modes, running mode and V2G mode. The vehicle battery can be charged from either solar power or grid power. The battery uses both power sources simultaneously when the power supply from solar source is not sufficient. The Integrated Power Converter acts as an isolated SEPIC converter during charging mode from grid power and as a non-isolated SEPIC converter in solar power charging mode. In propulsion and regenerative braking modes, it acts as boost topology and buck topology respectively. The Integrated Converter acts as a ZETA converter for Vehicle-to-Grid (V2G) mode. The main features of the proposed PEC are summarized as

- Dual sources for charging operation, which enhances reliability of the charger.
- Galvanic isolation for better safety of vehicle

users and charging circuit.

- Cheaper than conventional EV charger.
- Achieve all modes of vehicle.

The main objective of the paper is to carry out a study on the various topologies available for EV charging system and henceforth design and implement an integrated converter which can perform all modes of vehicle operation and powered from both solar PV system and grid power.

## 2. LITERATURE SURVEY

A plug-in electric vehicle is any road vehicle that can be recharged from an external source of electricity, such as wall sockets, and the electricity stored in the rechargeable battery packs drives or contributes to drive the wheels. Plug-in hybrid electric vehicles (PHEVs) use batteries to power the electric motor and another fuel, such as gasoline, to power an internal combustion engine (ICE). PHEV batteries can be charged using a wall outlet or charging equipment, by the ICE, or through regenerative braking.

A major feature of Electric Vehicles (EVs) is that they can be plugged in to an off-board electric power source for charging [1]. Off-board chargers are located outside the EVs. They can transfer higher units of power. This helps to charge the EVs faster. On the flipside, off-board chargers are heavier and larger. On-board charging systems are placed inside the vehicle and use AC supply. An on-board 3.3 KW charger can recharge a 16 KWH battery system to 95% in about 4 hours from a 240 V supply [2]. An on-board charger weighs less and is smaller.

Single stage charger is one type of on-board chargers, which directly transfers power from the AC source to the battery, thus eliminating the bulky electrolyte capacitor in a traditional two-stage charger. Since two-stage chargers require more components for charging, it is not widely used [3]. Single stage charging system requires only a few components and is hence cost effective. In [4], a quasi-two-stage charger has been proposed for a wide range of battery voltages. When the battery voltage is more than grid voltage, the proposed converter operates as the conventional boost converter (single-stage operation) and when the battery voltage is less than grid voltage, the battery takes power through

two stage operation; therefore, it is named as a quasi-two-stage converter. Two-stage operation results in lower efficiency of the converter. Also, this converter has slightly higher conduction losses than conventional boost Power Factor Correction (PFC) converter but it has lower switching losses due to its three-level output voltage characteristics.

In [5], an integrated converter has a buck/boost operation in each mode using three switches and two inductors (excluding filter inductor) in each mode. An integrated converter in [6] utilizes four switches and two inductors, has buck/boost operation only in plug-in charging mode. Moreover, this converter has high efficiency in propulsion and regenerative braking modes; therefore, the vehicle will cover longer distance for per charging.

The authors in [7] have proposed a compact OBC-based on CUK converter which operates in plug-in charging mode but this converter does not include other modes of vehicle operation. In [8], a SEPIC-based converter, using three inductors and at least one additional inductor is required to achieve propulsion and regenerative braking modes. Therefore, an increase in magnetic components will have a negative effect on weight, cost, and volume of the charger. In [9, 10], A SEPIC-based chargers for electric vehicle (EV) battery charging using a single-stage approach but they do not operate in other modes of vehicle. The authors in [11] have proposed a charger using four switches and two inductors which operates only in charging mode and does not operate in other modes of vehicle. Moreover, this converter has buck/boost operation during charging and low stresses on semiconductors.

A key requirement of an EV battery charger is that all power sources namely; solar PV and grid must be isolated from the battery [12], [13]. To charge the EV from solar PV and grid at least three converters are generally used [14]. First, a DC-DC converter is utilized for maximum power point tracking (MPPT) operation of the solar PV. The output solar PV (after MPPT) is connected to the output of grid interfaced converter (second converter), which forms a DC-link, and then a bidirectional DC-DC converter (third converter) is

connected between the DC-link and the battery [15], [16].

In conventional charging setup, a bidirectional DC-DC converter is placed between Inverter-DC link and battery in the running mode [17]. An integrated converter [18] which can perform all the functions by interfacing power supply and battery has been developed. It is desirable to charge the EVs from sustainable power sources. Hence charging of EVs from solar photovoltaic (PV) arrays is a viable option for the future [19]. Some of the topologies use plug-in charging mode and is not cost effective. The charger [20] uses only solar PV for charging the battery, when the solar power source is unable to generate the required power, leading to reduced system efficiency. The work [21] leads to the development of an integrated converter which uses both solar PV power and grid supply for charging.

When vehicles are parking for long duration, the battery is charged through solar PV charging, but the energy is not being used [22]. If this power is fed back to the grid, it will increase the efficiency of the entire system. With proper addition of controlled rectifier and utilization of bidirectional converter topology, energy can efficiently flow from vehicle to grid (V2G mode) [23]-[25].

Based on the above literature, a new dual-power single-stage multifunctional integrated converter is presented for EVs. The features of the integrated converter topology can be summarized as follows (a) It uses both solar and grid power for charging of battery, which increase the reliability of system. (b) It enhances the safety of the vehicle due to provision of isolation. (c) It is more cost effective due to reduction in the number of components. (d) It can achieve various modes of vehicle operation, and finally (e) The topology can use the solar power generated for implementation of V2G mode of operation.

### 3. MULTIFUNCTIONAL PEC

The integrated converter functions as a non-isolated and an isolated SEPIC converter during the two charging modes. It operates as a boost converter during propulsion mode and as a buck converter in

regenerative braking mode. The converter acts as an isolated ZETA during V2G mode of operation as shown in Fig.3. The semiconductor switches  $S_{a1}$ ,  $S_{a2}$ ,  $S_{a3}$  and  $S_{a4}$  control the charging and running modes by providing proper PWM. The mechanical switches  $P_1$ ,  $P_2$  and  $P_3$  are provided for proper mode selection.

### 3.1. Block Diagram of the Proposed Charger

The block diagram of the proposed system shown in Fig 3 consists of the two power supply sources – the grid and the PV. The integrated converter is connected to both sources for charging the battery.

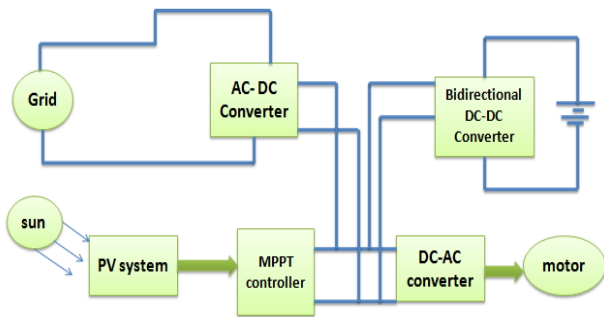


Fig.3: Block diagram of Proposed EV charging system

The integrated converter can perform multiple functions, AC–DC converter stage, MPPT controller, DC-AC inverter stage for motor running and finally it perform the functions of bidirectional converter.

### 3.2 Circuit Diagram Of The Proposed Converter

The circuit diagram of the topology is explained in Fig.4. The circuit consists of an integrated converter which can perform all modes of vehicle operation such as charging of battery from both the solar PV power and grid, running and Vehicle to grid (V2G) mode of operation. The circuit consists of four semiconductor switches  $S_{a1}$ ,  $S_{a2}$ ,  $S_{a3}$  and  $S_{a4}$  and three mechanical switches  $P_1$ ,  $P_2$  and  $P_3$  for the proper mode selection and operation.

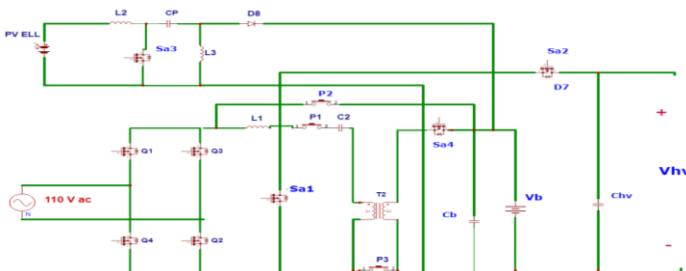


Fig.4: Circuit diagram of the integrated converter

## 4. MODES OF OPERATIONS

The system can achieve all modes of vehicle operation by using the proposed integrated converter. The operating modes of the proposed PEC are discussed in detail. States of the switching devices are shown in Table 1.

Table -1: Switching states in operational modes

Mode of operation	Sa1	Sa2	Sa3	Sa4	P1	P2	P3
Grid mode	PWM	OFF	OFF	OFF	ON	OFF	OFF
Solar PV mode	OFF	OFF	PWM	OFF	ON	OFF	OFF
Solar PV and grid mode	PWM	OFF	PWM	OFF	ON	OFF	OFF
PP mode	PWM	ON	OFF	OFF	OFF	ON	ON
RB mode	OFF	OFF	OFF	OFF	OFF	ON	ON
V2G / V2H mode	OFF	OFF	OFF	PWM	ON	OFF	OFF

### 4.1 Solar PV Mode

In situations where solar power is sufficient to charge the battery, it uses the Solar PV System to charge. The Solar PV system is connected to the battery through non-isolated SEPIC converter. The Perturb and Observer-based Maximum Power Point Tracking (MPPT) controller is implemented using dspic30f2010 through this non-isolated SEPIC converter for the optimal performance of the converter.

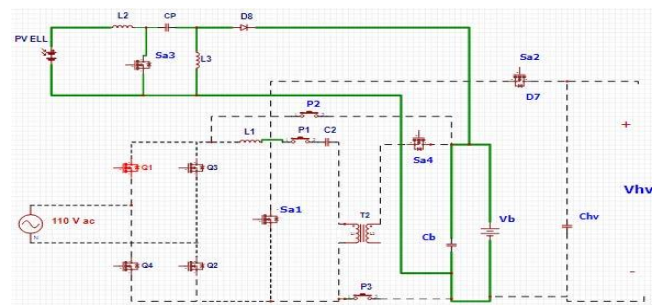


Fig.5: Solar PV Mode

When switch  $S_{a3}$  is turned ON, the solar power is supplied to inductor  $L_2$ .  $L_2$  stores the energy and capacitor  $C_p$  discharges its stored energy to inductor  $L_3$ . Thus inductors  $L_2$  and  $L_3$  are charging. During this time diode  $D_8$  is reverse-biased so that capacitor  $C_b$  provides sufficient energy to the battery. When  $S_{a3}$  is turned off,  $L_2$  charges capacitor  $C_p$  and  $L_3$  charges the battery through diode  $D_8$  which is forward-biased as shown in Fig. 5.

### 4.2 Grid Mode

When solar panel is unable to provide the required power for charging, the converter uses power from the grid. When switch  $S_{a1}$  turns ON, the active rectifier rectifies the AC voltage and the rectified DC voltage is given to  $L_1$  and  $C_2$  charges magnetizing inductance  $L_m$  of high frequency transformer and  $C_b$  provides the required energy for the battery. When  $S_{a1}$  is in OFF state, energy stored in  $L_m$  is transferred to the battery through diode  $D_6$  as shown in Fig. 6.

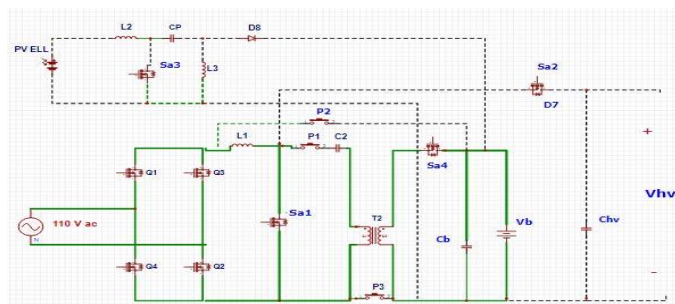


Fig.6: Grid Mode

### 4.3 Solar PV And Grid Mode

When solar power is not sufficient, grid power supports the charging of the battery. The grid supplies the remaining power. In this mode, battery is charged from both supplies simultaneously. The switches  $S_{a3}$  and  $S_{a1}$  control this mode.  $S_{a1}$  controls the charging of battery from grid power and  $S_{a3}$  controls the Solar Power charging of battery using proper PWM as shown in Fig.7.

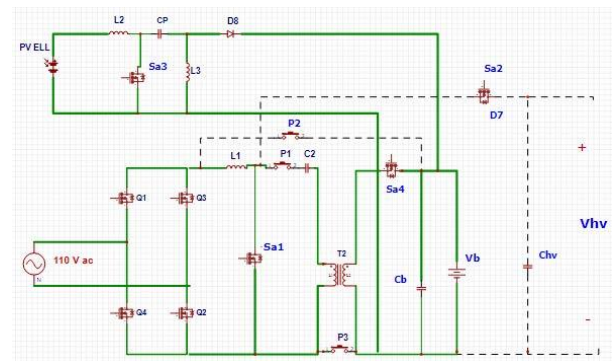


Fig.7: Solar PV and Grid Mode

### 4.4 Propulsion (PP) Mode

The system acts as a boost converter as the energy stored in the battery is boosted in to DC link voltage during the running mode. The switch  $S_{a2}$  controls the mode by giving the appropriate PWM signal. The mechanical switches  $P_2$  and  $P_3$  are permanently ON in this mode as shown in Fig.8. During turn ON of  $S_{a2}$ , the battery energy charges the inductor  $L_1$  and during turn off period,  $L_1$  discharges its stored energy to  $C_{hv}$ . This DC link voltage  $V_{hv}$  can be transferred to run the motor through an inverter setup.

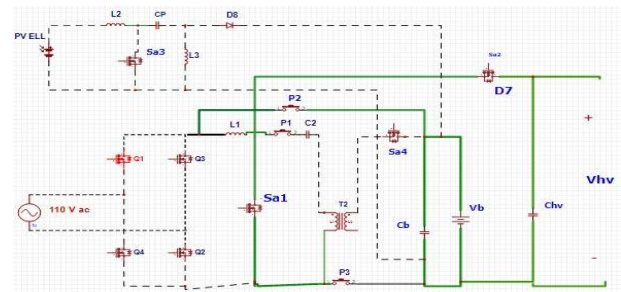


Fig.8: Propulsion Mode

### 4.5 Regenerative Braking (RB) Mode

The battery can be charged in running mode by using the kinetic energy of the wheels. Hence this mode is called RB mode. In this mode, the integrated converter is working as a buck converter. Switch  $S_{a2}$  controls the mode and  $P_2, P_3$  are permanently ON as in the propulsion mode. During turn ON period,  $L_1$  store the energy and this stored energy will be supplied to load during turn-off as shown in Fig.9.

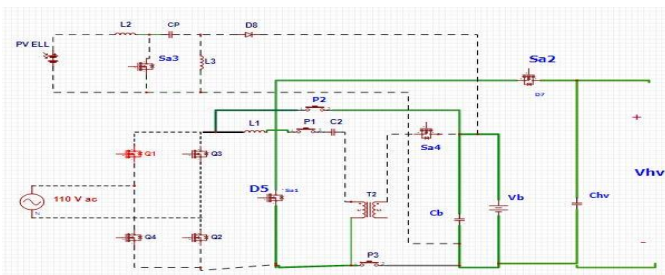


Fig.9: RB Mode

#### 4.6 vehicle To Grid (V2G)/Vehicle To Home (V2H) Mode

When charged vehicles are parked for long duration, energy stored in battery can be supplied back to grid, implementing V2G. The power converter acts as ZETA where switch  $S_{a4}$  controls this mode. During turn ON period of  $S_{a4}$ , capacitor  $C_s$  is charging and during the turn-off period, the energy stored in capacitor will be given to inductor  $L_{1s}$  as shown in Fig.10.

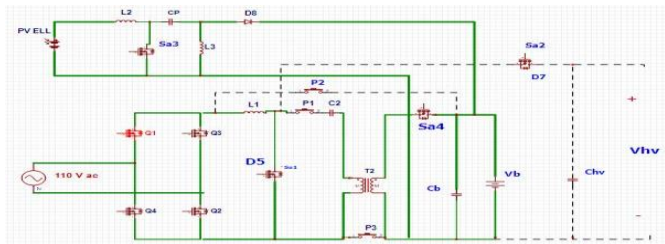


Fig.10: V2G Mode of Power Converter

#### 5. STRESS ON POWER DEVICES

The peak voltage and current stresses in the semiconductor power switches and diodes are necessary to determine the ratings of the power switches. The peak voltage and current stresses in switches for all modes are shown in Tables 2, 3. Based on peak stresses in the switches, the rating of the devices can be chosen.

Table -2: Voltage stress on semiconductor devices

Switching devices	Grid mode	PV mode	PP mode	RB mode	V2G mode
$S_{a1}$	$V_g + V_b$	-	$V_b$	$V_b$	-
$S_{a2}$	-	-	$V_{hv}$	$V_{hv}$	-
$S_{a3}$	-	$V_{pv} + V_b$	-	-	-

$D_6$	$V_g + V_b$	-	-	-	$V_g + V_b$
$D_8$	-	$V_{pv} + V_b$	-	-	
$S_{a4}$	-	-	-	-	$V_g + V_b$

The peak voltage stress is analyzed and tabulated in Table 2. Some of the semiconductor devices are made to operate and work in multiple modes, for example switch  $S_{a2}$  is operated in propulsion mode and in running mode. Hence the rating of the components is taken as the maximum rating as derived from Table 2. The voltage Stress on  $S_{a1}$  in PIC mode is  $(V_{g,max} + V_b)$  and in PP mode is  $V_b$ . Therefore, voltage rating of  $S_{a1}$  is can select based on PIC mode. The current rating of  $S_{a1}$  is also decided based on grid mode because current stress on the switch  $S_{a1}$  is the sum of the input output current. The switch  $S_{a2}$  conducts only in RB mode. The peak voltage developed across switch  $S_{a2}$  in RB mode is  $V_{hv}$ . Therefore, the voltage rating of  $S_{a2}$  is selected as  $V_{hv}$ . The current rating of  $S_{a2}$  is decided based on only RB mode. The voltage and current rating of switch  $S_{a3}$  is selected based on solar PV mode because  $S_{a3}$  conduct only in this mode.

#### 6. DESIGN OF PASSIVE COMPONENTS

In grid mode, the value of inductance can be calculated by analyzing the working of isolated SEPIC converter. The design part is as given below:

Table -3: Current stress on semiconductor devices

Switching Devices	Grid Mode	PV Mode	PP Mode	RB Mode	V2G Mode
$S_{a1}$	$i_g + < i_{Lm} > T_s$	-	$< i_{L1} > T_s$	-	$i_b + < i_{L1} > T_s$
$S_{a2}$	-	-	-	$< i_{L1} > T_s$	-
$S_{a3}$	-	$i_{pv} + < i_{L2} > T_s$	-	-	-
$S_{a4}$	$i_g + < i_{Lm} > T_s$	-	-	-	$i_b + < i_{L1} > T_s$

**a) Inductance**

Since the average voltage across an inductor is zero for periodic operation, the equations are combined to get

$$|V_g|(DT) - V_b((1-D)T) = 0$$

where D is the duty ratio of the switch. The result is

$$V_b = |V_g| \frac{D}{1-D}$$

which can be expressed as

$$D = d_1 = \frac{V_b}{V_b + |V_g|}$$

Solving for average inductor current, which is also the average source current,

$$V_{L1} = V_g = L_1 \frac{di_{L1}}{dt} = L_1 \frac{\Delta i_{L1}}{DT}$$

$$\Delta i_{L1} = \frac{V_g D}{L_1 f_s} \tag{1}$$

In PP mode, the value of inductance  $L_1$  can be calculated by analyzing the boost converter

$$V_{hv} = \frac{V_b}{(1-D)}$$

$$L_1 = \frac{V_b D}{f_s \Delta i_{L1}} \tag{2}$$

In RB mode, the value of  $L_1$  is calculated from equations given below

$$V_b = D V_{hv}; \quad D = d_2$$

From peak to peak inductor current, the value of  $L_1$  is summarized as

$$L_1 = \frac{V_{hv}(1-D)}{f_s \Delta i_{L1}}; \quad D = d_3 \tag{3}$$

In V2G mode of operation, the value of  $L_1$  can be found out from the expression

$$D = d_1 = \frac{V_g}{V_g + V_b}$$

$$L_1 = \frac{1}{2} \frac{V_b D}{f_s \Delta i_{L1}} \tag{4}$$

From these expressions of inductance  $L_1$  obtained from (1), (2) and (3), (4) the maximum value of  $L_1$  can be selected for the passive element  $L_1$ .

The value of magnetizing inductance  $L_m$  can be found out by using the expression

$$L_m = \frac{V_g^2}{P_g} \frac{1}{\epsilon f_s} \frac{V_b}{V_g + V_b}$$

Where  $\epsilon$  is % the ripple of the grid current  $i_g$ .

**b) Capacitances**

From the definition of capacitance and considering the magnitude of charge, solving for  $C_2$ ;

$$C_2 = \frac{V_b d_1(t)}{k V_g R_L f_s}$$

Where  $k$  is the % ripple in  $v_{cs}$  and  $R = \frac{V_b^2}{P_b}$

In V2G mode,  $C_2$  can be found out using the expression,

$$C_2 = \frac{i_g d_4}{\Delta V_g f_s}$$

The capacitor  $C_b$  is chosen based on second harmonic (100 Hz) voltage ripple experienced by it,

$$C_b = \frac{P_b}{2 \omega \delta V_b^2} \tag{6.2}$$

Where  $\delta$  is the ripple present and  $\omega = 2\pi f$  where  $f = 50\text{Hz}$

And  $C_b$  obtained from V2G mode (ZETA) is,

$$C_b = \frac{i_g d_4}{f_s \Delta V_g}$$

The value of capacitance  $C_{hv}$  is calculated by considering Propulsion mode, so that

$$C_{hv} = \frac{d_2}{R f_s} \frac{\Delta V_{hv}}{V_{hv}}$$

The non isolated SEPIC converter used for charging of battery from solar PV can be designed using the same analysis made in the previous section.

**7. COMPARATIVE ANALYSIS OF THE CONVERTER**

The proposed topology for EV charging uses an integrated converter which is analyzed and compared with several topologies. The comparative survey

include comparison with the existing topologies and life time and reliability analysis and finally loss analysis.

### 7.1 Comparative Evaluation with other Single Stage Charger Topologies

The proposed topology is compared with several single-stage chargers comprehensively in Table 4. In addition to these basic circuits, other integrated chargers using the same principle integration concept has been included in the comparative survey. As seen from Table 2, the proposed converter has the minimum number of semiconductor devices.

It requires only four semiconductor switches for all essential operation modes excluding V2G mode. For V2G mode the diode rectifier is replaced by an active rectifier which consist of 4 semiconductor switches.

### 7.2 Components Lifetime and Reliability Analysis

The lifetime of semi conductor switches are typically much higher. A failure during charging may affect the propulsion mode. Thus, the reliability of the proposed converter might slightly be lower than the conventional on-board chargers as two operation modes share the same components and some semiconductors are cycled more.

**Table -4:** Comparative analysis of proposed converter

Topology Reference No	Mode Of Operations					Number Of Switches
	Grid mode	PV	PP	RB	V2G / V2H	
[28]	Boost	-	Boost	Buck	-	4
[35]	Buck Boost	-	Boost	Buck	Buck	6
[29]	Buck Boost	-	Boost	Buck	-	6
[30]	Buck	Buck	Boost	Buck	Boost	8
[31]	Buck Boost	Buck Boost	-	-	-	15
[34]	Non Isolated Sepic	-	Boost	Buck	-	3
Proposed Converter	Isolated Sepic	Non Isolated Sepic	Boost	Buck	Zeta	4

### 7.3 Loss Analysis

Although the proposed converter has the minimum number of switches and circuit components, it slightly has higher conduction power loss compared to basic topologies. Nevertheless, there is no additional switching loss as only one power switch is switched in each operation mode. The total losses in plug in charging (ac/dc stage) and propulsion (dc/dc stage) modes of the proposed converter and with their conventional counterparts are given in Table 5, 6. Moreover, loss calculation of regenerative braking mode (dc/dc stage) has not been considered in this analysis because propulsion mode power rating is usually much higher compared to regenerative braking mode power rating; therefore, loss calculation of propulsion mode is sufficient to analyze the losses of regenerative braking mode. In the ac/dc stage, the proposed converter has one additional mechanical type switch, i.e.  $P_1$  compared to conventional SEPIC converter due to that there will be an efficiency drop in the proposed structure which varies between 0.1 and 0.45% for 1.1kW and 2.9kW charging power.

In the dc/dc stage with power rating 800 W, 65kW efficiency drop is 1.175, 1.33% respectively, compared to the conventional boost converter. In the dc/dc stages, two additional devices ( $S_{a2}$  or  $S_{a3}$  and  $P_2$  and  $P_3$ ) are in the current path on the other hand, in the ac/dc stage only one additional device ( $P_1$ ) is in the current path compared to their conventional counterparts; therefore, percentage increase of losses in dc/dc stage will be higher compared to ac/dc stage. Moreover, in the proposed converter, there is no additional switching loss in any mode compared to conventional converters.

## 8. CONTROL TECHNIQUES

Control techniques of the integrated modes are explained in this section. various control techniques define the mode of operation by giving PWM for switches. The control techniques used for charging (Solar PV , grid mode ) and running ( PP and RB ) and V2G modes are explained below.

**Table -5:** Loss analysis of proposed converter during grid mode

Grid Mode				
Grid Supply	Battery Specifications	Total Losses		Efficiency Drop (%)
110 V , 10 A	48V ,800 W	49	54	0.1
230 V , 13A	320 V ,65 KW	419.74	455	0.45

**8.1 Control Technique for Grid and Solar PV Modes**

The battery is charged from both Solar PV and the grid, with priority to solar power. It is a two-loop control strategy. The energy supplied by the grid is calculated using the error detector and the output is fed to the PI controller. The DC signal produced by the PI controller is compared with the sawtooth waveform and the pulse generated is given to switch Sa1 to control the grid mode as shown in Fig.11.

**Table -6:** Loss analysis of proposed converter during PP mode

PP Mode				
Grid Supply	Battery Specifications	Total Losses		Efficiency Drop (%)
110 V , 10 A	48V ,800 W	34.6	44	1.175
230 V , 13A	320 V ,65 KW	656.91	1526.73	1.33

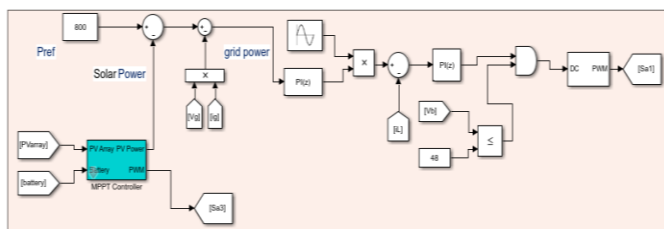


**Fig.11:** Control of Solar PV and Grid Modes

**8.1.1 Fuzzy Logic Controller**

In this section the MPPT controller is developed using Fuzzy logic controller to track MPP of PV system. The MPPT Fuzzy controller has two inputs such as PV Voltage and PV current, The MPPT Fuzzy controller

generates a duty cycle based on input of Fuzzy controller and is fed to SEPIC converter.

**8.1.2 P &O Algorithm**

The solar mode is controlled using Perturb and Observer-based algorithm as shown in Fig.12. Microcontroller based charge controller design is feasible for performing complex tasks. dspic30F2010 microcontroller used in this charge controller is central in coordinating all system activities. Port A is used for voltage sensing of battery and solar voltage whereas port B controls disconnect or reconnect operations for PV panel or load. Port B also controls generation of PWM signal which in turn controls the SEPIC converter as shown in the electrical schematic diagram Fig.13.

**8.2 Control Technique For PP and RB Modes**

The control technique for PP and RB modes are shown in Figure.10. Maintaining a constant DC link voltage is the purpose of PP mode. There are outer loop and inner loop controls as shown in Fig. 14. The outer loop of both the modes produce reference battery current. It is compared with the actual battery current and the error signal is fed to the inner PI controller. The controller produces DC signal which is compared with a sawtooth signal produced by high frequency sawtooth generator and the generated pulse is provided to switch Sa2.

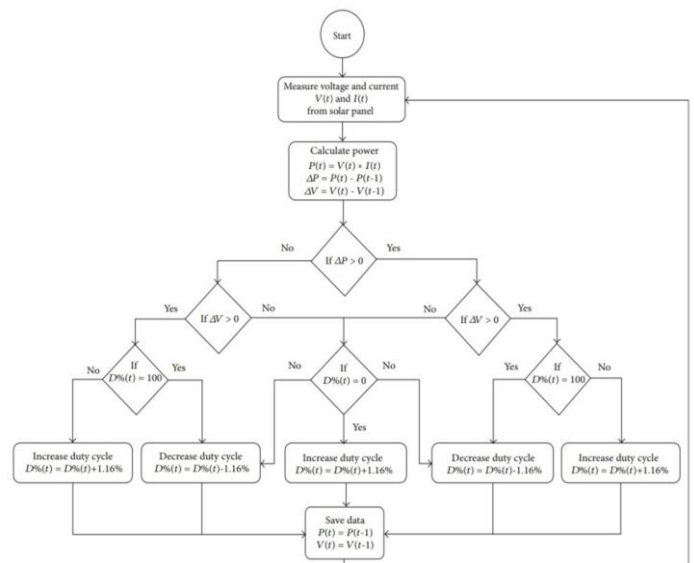


**Fig.12:** Flow chart of P &O MPPT algorithm

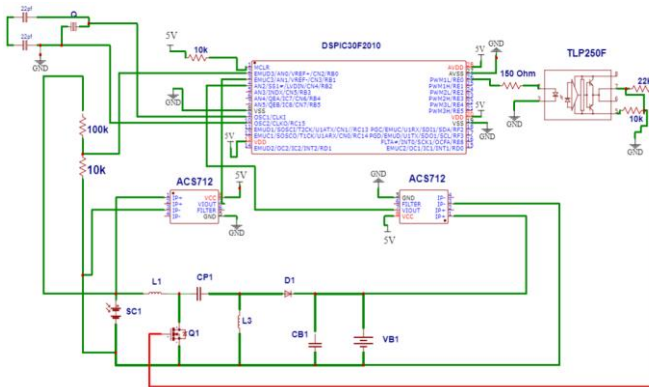


Fig.13: Electrical schematic of MPPT controller

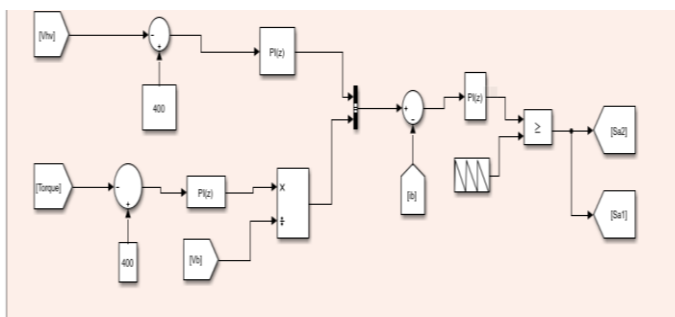


Fig.14: Control of PP and RB Modes

### 8.3 Control Technique for V2G /V2H Mode

The control strategy is a two-loop technology. The outer loop compares the actual and the reference voltages of the battery and the error is given to the outer PI controller which produces the reference current for V2G operation. The flow chart indicating V2G/V2H mode is shown in Fig.15. If solar power is more than required power of the battery, then V2G/V2H operation is possible, i.e.  $P_{pv} - P_{ev}$  will be supplied back to the grid or can be used for residential load. The error detector feeds the difference between the measured and the reference battery currents to the inner PI controller which produces PWM signal for the operation as shown in Fig. 16.

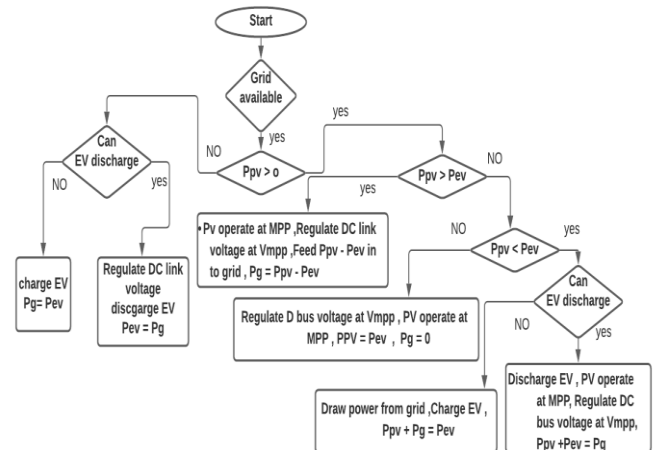


Fig.15: Flow Chart indicating V2G Mode

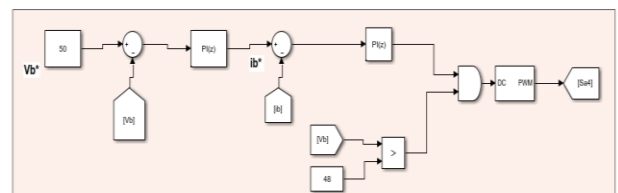


Fig.16: Control of V2G Mode

## 9. RESULTS AND DISCUSSIONS

The integrated power converter is simulated on MATLAB SIMULINK 2018 software and the results are validated for a 48 V, 26 Ah battery and a DC link voltage of 150V. The table 7 explains the two sets of parameters used for simulation as obtained from design section. All modes are simulated and results are explained below.

### 9.1 Simulink Diagram

The simulink diagram of the proposed EV charger for different modes of operations are shown in Fig.17.

#### 9.1.1 Simulink Diagram Of Perturb And Observe Based Algorithm

The Perturb and Observation (P&O) algorithm is a tracking technique algorithm used in MPPT to achieve maximum power by perturbing the power source and observing the impact. There are various MPPT algorithms, such as fuzzy logic and particle swarm optimization. However, P&O is the most used technique in an MPPT system because it has a simple algorithm and does not require a high capability controller

device. The first step of the P&O algorithm is measuring the voltage and current of the solar module, then calculating the current value and the difference between the current voltage and power against voltage and power measured from the previous loop. The controller then decides, from the difference value, whether to increase or decrease the voltage of the solar module by changing the duty cycle of the PWM signal so that the power of the solar module will increase.

### 9.2 Simulation Results of Operational Modes

The simulation is carried out for two sets of designed values and the results are obtained for each mode of operation and are discussed below.

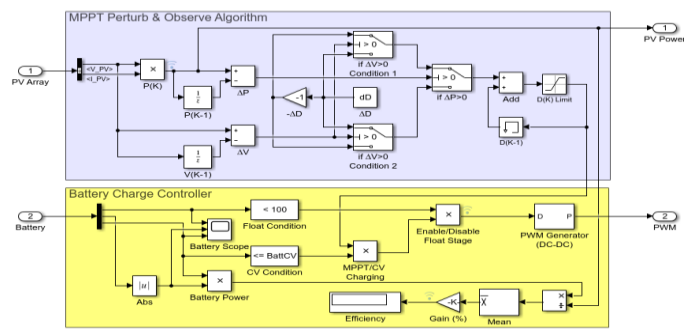


Fig.18: Simulink diagram of P&O algorithm

The measured battery current in this mode is 16 A and power at battery side is 800 W. The overall efficiency of both converters (SEPIC isolated and SEPIC non-isolated) is 90.6%.

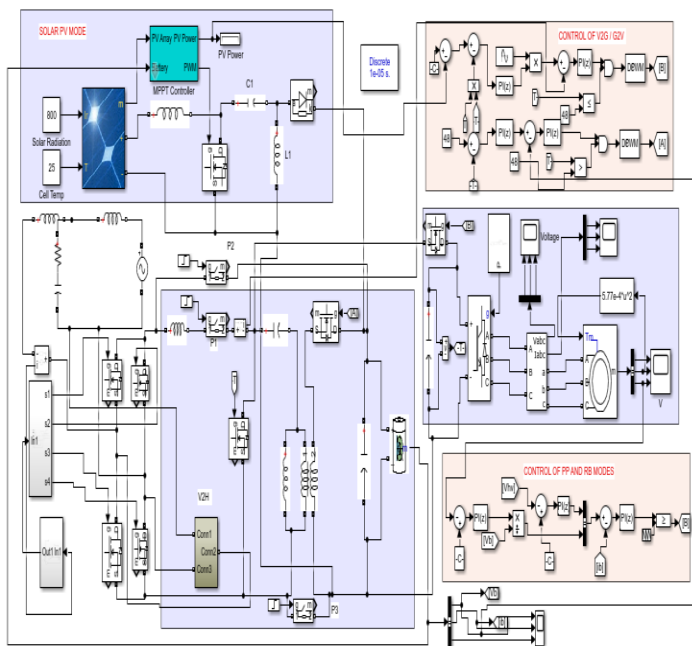


Fig.17: Flow Chart indicating V2G Mode

#### 9.2.1 Solar PV Mode

When Solar PV alone supplies the required power to the battery, the measured Solar PV voltage at Maximum Power Point (MPP) is 60 V and current is 12 A, as shown in Fig. 19. The battery voltage and battery current are shown in Fig. 20.

Parameters	Values
Grid voltage ( Vg)	110 V
Dc link voltage (Vhv)	400 V
Reference power	800 W
Line frequency	50 Hz
Switching frequency (fsw)	20 kHz
Battery voltage (Vb)	48 V
Capacity	26 Ah
L1, L2 , L3 , Lm	2,2,2,2 mH
Chv, Cs, Cb	330 μF, 1 μF, 1200 μF
Motor specifications	Rotor type – squirrel cage, 3 HP, 230 V, 50 Hz
Inverter (motor side)	3 phase full bridge inverter m=0.9 Frequency=18*50

Table -6: Simulation Parameters

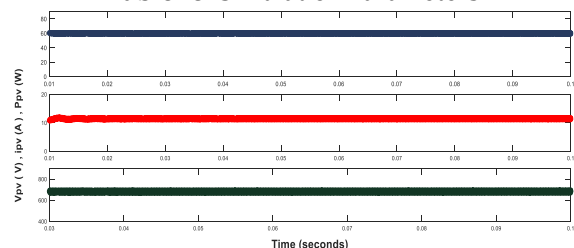


Fig.20: Solar PV voltage and current waveform

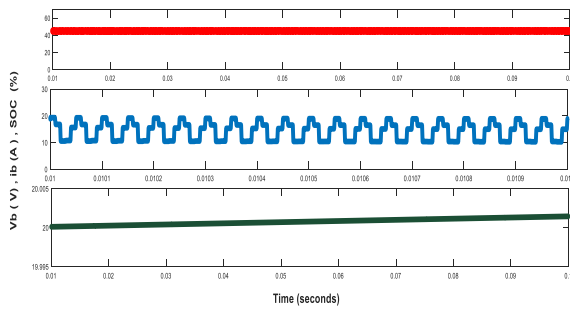


Fig.20: Battery voltage and current waveform

### 9.2.2 Fuzzy Logic Controller Based PV Mode

The MPP of Solar Power using Fuzzy Logic Controller is simulated on MATLAB and simulink diagram and the corresponding waveforms for 48 V , 26 Ah Battery are shown in fig. 21. and fig .22 and 23.

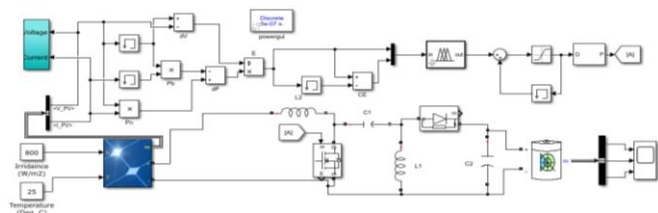


Fig.21: Simulink Diagram of Fuzzy Logic controller based Solar PV Mode

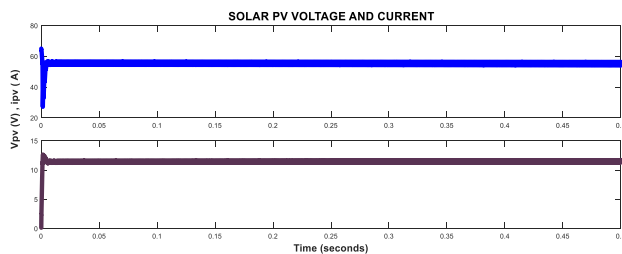


Fig.22: Solar PV voltage and current waveform

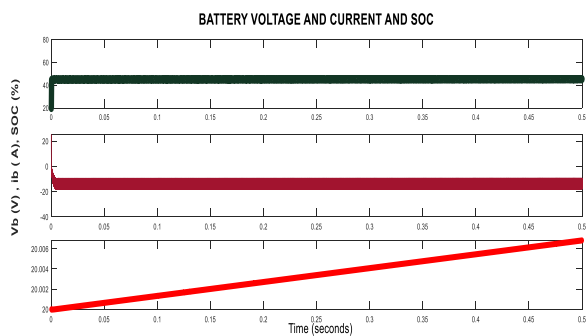


Fig.23: Battery voltage and current waveform

### 9.2.3 Grid Mode

If solar system is unable to generate required power, then grid is supplying the required power for charging of battery. The simulation is carried for 110 V /10A, AC supply. For the AC grid supply of 1.1 kW power the battery is charging with a voltage of 48 V and 15.5 A and the efficiency is calculated as 93% for 800 W reference power.

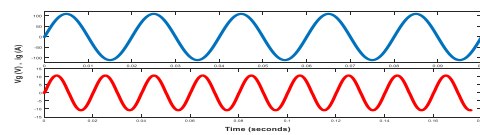


Fig.24: Grid voltage and current waveform

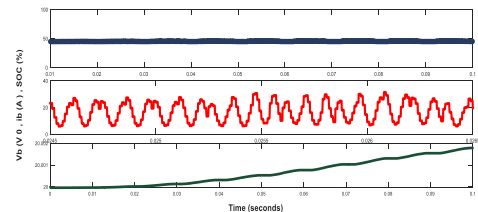


Fig.25: Battery voltage and current waveform

### 9.2.4 Diesel Generator (DG) Set Based Battery Charger

The DG set is feeding load, for the analysis of the efficiency with grid mode is simulated. In this condition, the DG set is always operated at 80-85% of the loading so that the efficiency of the diesel engine remains maximum. A 100kW DG set is generating 98 kW electrical energy.

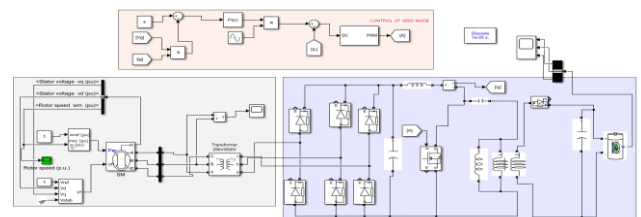


Fig.26: Simulink diagram of DG set based integrated converter

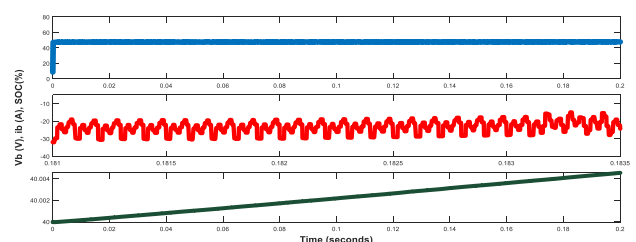


Fig.27: Battery voltage and current waveform

### 9.2.5 Solar PV and Grid Mode

In Solar PV and Grid mode, Solar PV system is set to operate at 400 W/ m<sup>2</sup> solar irradiation, and the reference power is set as 800 W. Here solar PV system provides 400 W and the remaining power is supplied by the grid. The grid voltage and current  $V_g$  and  $i_g$  are in the same phase as shown in Fig. 28.

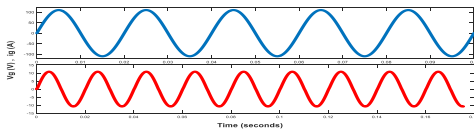


Fig.28: Grid voltage and current waveform

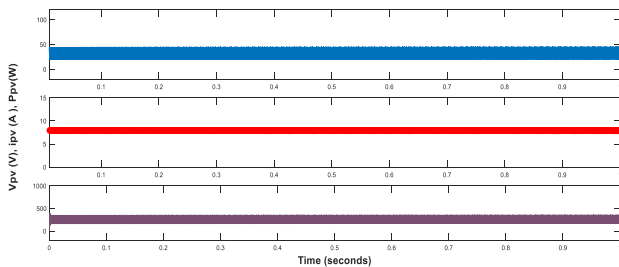


Fig.29: Solar PV voltage and current waveform

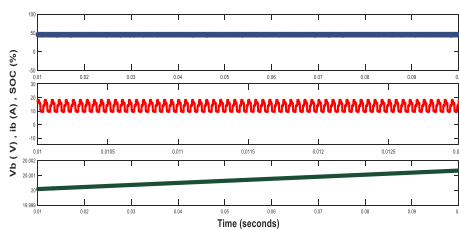


Fig.30: Battery voltage and current waveform

The measured Solar PV voltage at Maximum Power Point (MPP) is 48 V and current is 9 A. The Solar PV power, voltage and current are shown in Fig.29. The measured battery current in this mode is 15 A and power at battery side is 750 W as shown in Fig.30. The overall efficiency of both converters (SEPIC isolated and SEPIC non-isolated) is 93.75%.

### 9.2.6 Isolated Zeta Based Grid Mode

To compare the efficiency of the proposed integrated converter, the isolated SEPIC converter during grid mode is replaced by isolated ZETA converter and the design steps are made for the ZETA and the simulation is carried out on MATLAB. The simulink diagram and the corresponding waveforms are shown below.

### 9.2.7 Propulsion and Regenerative Braking Modes

The reference DC-link voltage is 400 V and the objective of PP mode is to regulate the DC-link voltage at the reference value. The corresponding DC link voltage and SOC of battery waveforms are shown in Fig.32. The speed of the motor decreases when brakes are applied. Hence the generated voltage, i.e., DC link voltage decreases. This regenerative braking mode is tested by reducing DC link voltage from 400 V to 250 V.

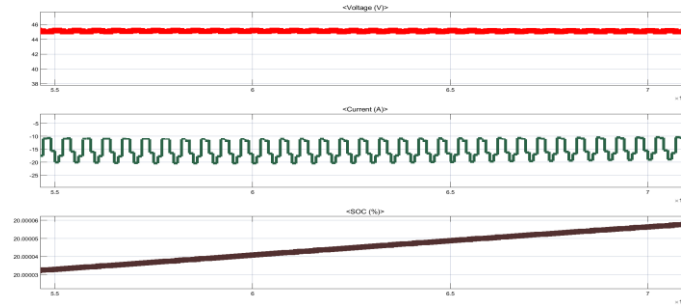


Fig.31: Battery voltage and current waveform

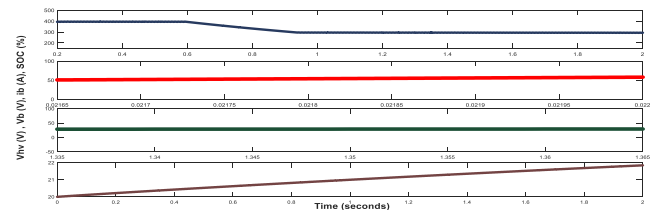


Fig.32: DC link voltage and battery discharging in PP mode

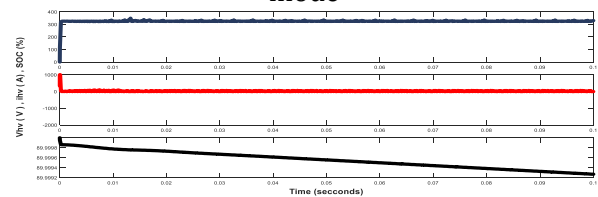


Fig.33: Battery charging in RB mode

The battery is charged through a current of 20 A and voltage of 50 V as shown in Fig. 33. The THD of the inverter output voltage is shown in Fig.35. and motor parameters are shown in Fig.34.

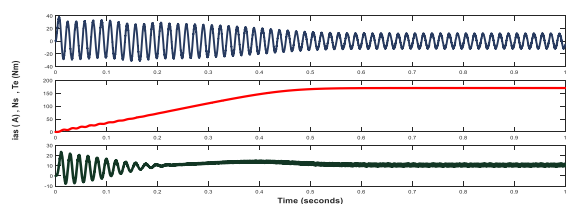


Fig.34: Battery charging in RB

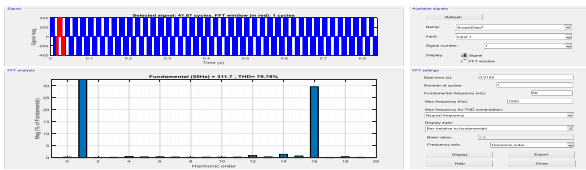


Fig.35: THD of inverter line to line voltage

9.2.7 V2G /V2H Mode

The energy stored in battery during parking period is utilized for V2G operation. The simulation is carried out by controlling the semiconductor switch Sa4 by giving a proper PWM signal, and the waveforms obtained are shown in Fig.36.

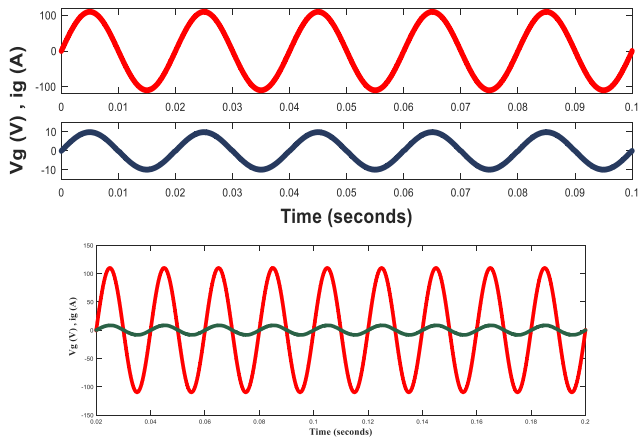


Fig.36: Grid voltage and current waveform during V2G mode

The Total Harmonic Distortion (THD) of the grid current have been shown in Fig.37. The THD of the grid current is found as 1.87% and PF is unity. Which indicates converter is drawing almost negligible reactive power. V2H mode is implemented using an asynchronous machine as load. The asynchronous machine is controlled by a square relation between the rotor speed and the mechanical torque which is shown in Fig.38.

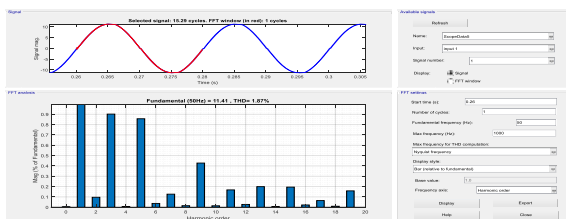


Fig.37: THD(%) in Grid current

9.3 Analysis of Simulation Results

From the simulation results obtained in the previous section we can analyze the performance of each mode of operation and its efficiency. The analysis is carried out for all modes of operations and results obtained are tabulated as shown in table 6.

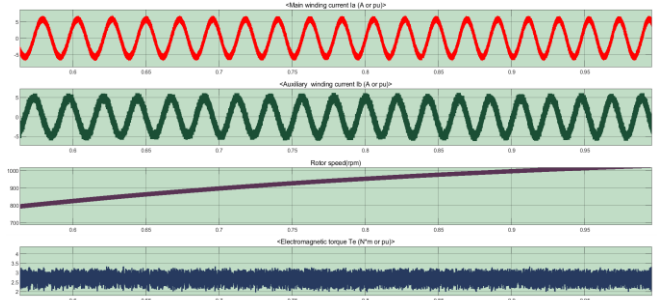


Fig.38: Asynchronous machine as load in V2H Mode

From the table it is clear, which mode highest efficiency and how much .Solar PV and Grid mode has higher efficiency than that of individual modes of solar PV and Grid mode. The THD of current in V2G mode and voltages of inverter in running mode is estimated using FFT analysis and are tabulated. It is noted that the efficiency of Solar PV and Grid mode is more compared to independent charging of solar PV

Table -6: Analysis of Simulation Results

Algorithm Used	Solar PV mode			
	Reference power	Solar panel specification	Battery specification	Efficiency (%)
P & O	800 W	60V, 12A	48 V, 15A	90
Fuzzy Logic	800W	58V, 12A	48V, 15A	90
AC Supply	AC Mains			
	Reference Power	AC supply	Battery Specification	Efficiency (%)
DG Set	1300W	400 V	48V, 25A	92.3
Grid Supply	800W	110V, 10A	48V, 15.5A	93
Solar PV and Grid Mode				
Solar Panel Specification	Reference power	Grid Supply Specification	Battery Specification	Efficiency (%)

		on		
48V,8A	800W	110V,10A	50V,15A	93.75
<b>PP Mode</b>				
Reference Voltage	DC Link Voltage		Efficiency	
400V	350V		87.5	
<b>RB Mode</b>				
Reduction in DC Link Voltage	Battery Specification	THD (%)in motor Line to Line Voltage		
400V to 250 V	50V,25A	79.78		
<b>V2G /V2H Mode</b>				
Grid Voltage and Current	Battery specification	THD(%)in Grid current		
110 V,10A	320V ,200Ah	1.87		

mode and grid mode .so the efficiency and the reliability of the system can be increased by using dual power sources .It is clear that the efficiency of the propulsion mode is less compared to other operational modes (charging ) which validate the loss analysis carried out in section .

In the ac/dc stage, the proposed converter has one additional mechanical type switch, i.e.P<sub>1</sub> compared to conventional SEPIC converter due to that there will be an efficiency drop , so the efficiency is seem to be 92.3% and 90 for 1.3 kW and 40 kW reference power. In the dc/dc stage the efficiency is found as 87.5% for 400 V reference power. In the dc/dc stages, two additional devices (P<sub>2</sub> and P<sub>3</sub> ) are in the current path on the other hand, in the ac/dc stage only one additional device (P<sub>1</sub>) is in the current path compared to their conventional counterparts; therefore, the efficiency of PP mode is slightly less compared to charging mode.

### 10. CONCLUSION

In this paper, a new Integrated Power Converter is introduced and its various modes of operation are discussed. The Converter can operate in various modes of vehicle operation and the topology is simulated using the parameters obtained from the analysis of the converter. The results are verified for two sets of

simulation parameters of 800 W reference power and grid supply of 110 V / 10 A and battery capacity of 48 V, 26 Ah and 230 V/13 A grid supply and 320 V, 200 Ah lead acid battery. The solar PV mode is simulated using both P&O algorithm and Fuzzy logic controller and the efficiency is compared. The efficiencies of various modes are analyzed. The grid mode is simulated for both SEPIC converter and ZETA converter and it is seem to charging via SEPIC converter is more compared to ZETA. The topology is working as SEPIC converter during its charging, as conventional boost and buck converters during running modes. The charge in the battery during long parking periods is used to implement V2G operation and this is achieved by working the converter as a ZETA. Various modes of operations and analysis of converter stages are carried out and designed values of parameters are used for simulation using MATLAB 2018 and each mode is controlled using the methods described in chapter 8. The efficiency of each mode is calculated from the simulation results.

By the integration of more number of vehicles and proper control, the V2G mode can be extended to three phase grid integration system. A diesel generator set can be added as the power supply to increase the reliability by addition of a synchronizing switch is used between grid/DG set and PCC for controlled connection/ disconnection of charging station to grid/DG set.

### REFERENCES

- [1] M. Yilmaz and P. T. Krein, "Review of battery charger topologies, charging power levels, and infrastructure for plug-in electric and hybrid vehicles," IEEE Trans. Power Electron., vol. 28, no. 5, May 2013.
- [2] Gautam, Deepak, FariborzMusavi, MurrayEdington, Wilson Eberle and William G. Dunford."An Automotive OnBoard 3.3 kW Battery Charger for PHEV Application." IEEE Transactions on Vehicular Technology (61) 8, October 2012.
- [3] A.V. J. S. Praneeth and S. S.Williamson, "A wide input and output voltage range battery charger using buck-boost power factor correction converter,"in Proc. IEEE Appl. Power Electron. Conf. Expo., Mar. 2019.

- [4] Tang, Y., Zhu, D., Jin, C., et al.: "A three-level quasi-two-stage single-phase PFC converter with flexible output voltage and improved conversion efficiency", IEEE Trans. Power Electron., 2015.
- [5] Singh, A.K., Pathak, M.K.: "Single-stage zeta-sepic-based multifunctional integrated converter for plug-in electric vehicles", IET Electr. Syst. Transp., 2018.
- [6] Singh, A.K., Pathak, M.K.: "A multi-functional single-stage power electronic interface for plug-in electric vehicles application", Electr. Power Compon. Syst., 2018.
- [7] Patil, D., Sinha, M., Agarwal, V.: "A Cuk converter based bridgeless topology for high power factor fast battery charger for electric vehicle application". 2012 IEEE Transportation Electrification Conf. and Expo (ITEC), Dearborn, MI, USA, 2012.
- [8] Kong, P.Y., Aziz, J.A., Sahid, M.R., et al.: "A bridgeless PFC converter for on-board battery charger". 2014 IEEE Conf. on Energy Conversion (CENCON), Johor Bahru, Malaysia, 2014.
- [9] Maharjan, M., Tandukar, P., Bajracharya, A., et al.: "Sepic converter with wide bandgap semiconductor for pv battery charger". 2017 Brazilian Power Electronics Conf. (COBEP), 2017, Juiz de Fora, Brazil.
- [10] Dadashzadeh, H., Khosroshahi, A.E., Hosseini, S.H.: "A digital predictive controller for a sepic-based battery charger in photovoltaic power systems". 2017 IV Int. Electromagnetic Compatibility Conf. (EMC Turkiye), Ankara, Turkey, 2017.
- [11] Oh, C.Y., Kim, D.H., Woo, D.G., et al.: "A high-efficient nonisolated single stage on-board battery charger for electric vehicles", IEEE Trans. Power Electron., 2013.
- [12] CHAdeMO Association, "Technical specifications of quick charger for the electric vehicle," CHAdeMO Protoc. Rev. 1.1, 2010.
- [13] SAE Electric Vehicle and Plug-in Hybrid Electric Vehicle Conductive Charge Coupler, SAE Std. J1772, 2010.
- [14] R. Bhatti, Z. Salam, M. J. B. A. Aziz, K. P. Yee, and R. H. Ashique, "Electric vehicles charging using photovoltaic: Status and technological review," Renewable and Sustainable Energy Reviews, vol. 54, 2016.
- [15] G. R. C. Mouli, P. Bauer, and M. Zeman, "Comparison of system architecture and converter topology for a solar powered electric vehicle charging station," in 2015 9th International Conference on Power Electronics and ECCE Asia (ICPE-ECCE Asia), pp. 1908–1915, Jun. 2015.
- [16] A.K. Singh and M. K. Pathak, "A multi-functional single-stage power electronic interface for plug-in electric vehicles application," Electric Power Components and Systems, vol. 46, 2018.
- [17] A. K. Singh and M. K. Pathak, "Integrated converter for plug-in electric vehicles with reduced sensor requirement," IET Elect. Syst. Transp., vol. 9, no. 2, pp. 75–85, 2019.
- [18] S. Dusmez and A. Khaligh, "A charge-nonlinear-carrier-controlled reduced-part single-stage integrated power electronics interface for automotive applications," IEEE Trans. Veh. Technol., vol. 63, no. 3, pp. 1091–1103, Mar. 2014.
- [19] G. R. C. Mouli, P. Bauer, and M. Zeman, "Comparison of system architecture and converter topology for a solar powered electric vehicle charging station," in 2015 9th International Conference on Power Electronics and ECCE Asia (ICPE-ECCE Asia), Jun. 2015.
- [20] S. Biswas, L. Huang, V. Vaidya, K. Ravichandran, N. Mohan, and S.V. Dhople, "Universal current-mode control schemes to charge Li-ion batteries under DC/PV source," IEEE Trans. Circuits Syst. I: Reg. Papers, vol. 63, no. 9, pp. 1531–1542, Sep. 2016.
- [21] G. R. C. Mouli, J. Schijffelen, M. van den Heuvel, M. Kardolus, and P. Bauer, "A 10 kw solar-powered bidirectional EV charger compatible with chademo and combo," IEEE Trans. Power Electron., vol. 34, no. 2, Feb. 2019.
- [22] Ankit Kumar Singh, "A Multifunctional Solar PV and Grid Based On-Board Converter for Electric Vehicles", IEEE transactions on vehicular technology, vol. 69, no. 4, April 2020
- [23] M. J. E. Alam, "Effective Utilization of Available PEV Battery Capacity for Mitigation of Solar PV Impact and Grid Support With Integrated V2G Functionality", IEEE transactions on smart grid, 2015.
- [24] Mithat C, "EV/PHEV Bidirectional Charger Assesment for V2G Reactive Power Operation", IEEE Transaction on power electronics, 2013.
- [25] Zheng Wang, "An integrated power conversion system for electric traction and V2G Operation in Electric Vehicles With A Small Film apacitor", IEEE power electronics regular paper, 2019.

- [26] L Umanand, "power electronics essentials & applications", centre for electronic design & technology, Indian institute of science, 2009.
- [27] Bhim Singh, "Implementation of Solar PV-Battery and Diesel Generator Based Electric Vehicle Charging Station", IEEE Transactions on Industry Applications, 2020.
- [28] S. Dusmez and A. Khaligh, "A charge-nonlinear-carrier-controlled reduced-part single-stage integrated power electronics interface for auto motive applications," IEEE Trans. Veh. Technol., vol. 63, no. 3, Mar. 2014.
- [29] S. Dusmez and A. Khaligh, "A compact and integrated multifunctional power electronic interface for plug-in electric vehicles," IEEE Trans. Power Electron., vol. 28, no. 12, Dec. 2013.
- [30] Anjeet Verma, "An Implementation of Solar PV Array Based Multifunctional EV Charger", IEEE Transactions on Industry Applications, 2020.
- [31] Gautham Ram Chandra Mouli, "A 10kW Solar-Powered Bidirectional EV Charger Compatible with Chademo and COMBO", IEEE Transactions on Power Electronics, 2018.
- [32] Kai-Wei Hu, "An EV SRM Drive Powered by Battery/ Super capacitor with G2V and V2H/V2G Capabilities ", IEEE transactions on industrial electronics, 2015.
- [33] Yi-Chun Hsu, "On an Electric Scooter with G2V/V2H/V2G and Energy Harvesting Functions", IEEE Transactions on Power Electronics, 2017.
- [34] Tomy Abuzairi, "Solar charge Controller with Maximum power point tracking for low power solar applications", International Journal of Photo Energy, 16 Dec 2019.
- [35] O. C. Omar, J. Kobayashi, D. C. Erb, and A. Khaligh, "A bidirectional high-power-quality grid interface with a novel bidirectional non inverted buck-boost converter for PHEVs," IEEE Trans. Veh. Technol., vol. 61, Jun. 2012.